




Poly(ionic liquid)s-based polyurethane blends: effect of polyols structure and ILs counter cations in CO₂ sorption performance of PILs physical blends

Murilo da Luz^{1,2} · Guilherme Dias^{1,2} · Henrique Zimmer¹ · Franciele L. Bernard¹ · Jailton F. do Nascimento³ · Sandra Einloft¹ 

Received: 6 December 2020 / Revised: 14 May 2021 / Accepted: 22 June 2021 /
Published online: 28 June 2021

© The Author(s), under exclusive licence to Springer-Verlag GmbH Germany, part of Springer Nature 2021

Abstract

Carbon dioxide (CO₂) capture from natural gas, and further utilization is an essential issue for greenhouse gas reduction. Poly(ionic liquid)s (PILs) assemble ILs unique properties, with those of polymers being versatile materials for CO₂ capture from flue gas (CO₂/N₂) and natural gas (CO₂/CH₄). PILs based on polyurethanes obtained with different polyols and ILs cations were blended in different proportions aiming to improve PILs CO₂ sorption capacity. Two different polyols structures (PC and PG) and ILs counter cations (imidazolium and phosphonium) were tested to evaluate how they influence PILs blends CO₂ sorption performance. PILs and PILs blends were characterized by SEC, FTIR, DSC, TGA, DMTA, AFM, and CO₂ sorption that were carried out using the pressure-decay technique. PILs blends presented good thermal stability and mechanical properties. PILs blend polyurethane backbones compositions can be tuned aiming to increase CO₂ sorption capacity. As far as we know, all obtained PILs blends presented higher CO₂ sorption capacity results compared with other Poly(ionic liquid)s reported in the literature. The best CO₂ sorption result was obtained for PIL blend with imidazolium (PLIPC95-PG5-BMIM = 116.9 mgCO₂/g at 303.15 K and 10 bar).

Keywords CO₂ capture · Poly(ionic liquid)s · Blends · Polyurethane

✉ Murilo da Luz
einloft@pucrs.br

¹ School of Technology, Pontifical Catholic University of Rio Grande Do Sul (PUCRS), Avenue Ipiranga, 6681, Partenon, Porto Alegre CEP: 90619-900, Brazil

² Post-Graduation Program in Materials Engineering and Technology, Pontifical Catholic University of Rio Grande Do Sul (PUCRS), Porto Alegre, Brazil

³ Petrobras/CENPES, Ilha do Fundão Qd. 07, Rio de Janeiro, RJ, Brazil

Introduction

Carbon dioxide (CO₂) recovery from industrial waste gases is of great importance for further utilization and from an environmental point of view [1–3]. Conventional absorption technologies using amines aqueous solutions for capturing CO₂ have as main limitations the corrosivity, volatility, degradation, and high energy consumption. Therefore, the development of new technologies is necessary [4]. Ionic liquids (ILs) have unique physico-chemical properties as CO₂ high solubility and selectivity, low volatility, among others. Compared to conventional organic solvents, ILs present high thermal resistance and less toxicity to the environment. However, ILs high viscosity and cost and low CO₂ sorption/desorption rates, compared to amine solutions, restrain its application for CO₂ capture [5–9]. To solve the high viscosity and cost drawbacks, ILs can be incorporated into polymeric chain-forming Poly(ionic liquid)s (PILs). These materials present better performances for CO₂ capture once compared to bare ILs [4, 10, 11]. PILs combine the good ILs and polymers properties, increasing the range of applications of these materials in different areas [5, 12–14]. To date, the PILs classes obtained through condensation reaction and tested to CO₂ capture reported in the literature are: polyimides [15–17], polyesters [18], polybenzimidazoles [19, 20], polyurethanes [3, 7, 21–23], polyepoxydes [24–26]. These functional polymers can be applied as alternative solid sorbents for CO₂ capture and separation. Several studies have investigated the CO₂ sorption capacity of PILs with promising results [3, 7, 22, 27–38]. PILs typically present higher CO₂ sorption capacity when compared to the corresponding ILs [30, 39]. Yet, the sorption/desorption process is faster and completely reversible [4, 10, 28, 40]. In addition, PILs have better selectivity for separating CO₂ from other gases [9, 41, 42]. Membranes for gas separation are used to separate certain gases, such as CO₂, from gas streams in different systems [4, 8]. Polymeric membranes have some advantages, such as good mechanical properties, low cost, synthetic viability, and large-scale production, appearing as an option for gas separation processes [43, 44]. However, polymeric membranes commonly present problems associated with low permeability or low selectivity [45]. A method to improve polymers properties is the blend formation [46]. Polymer blends are being increasingly used in the development of new materials [47]. Blends have become an ideal method for obtaining polymeric membranes with high mechanical properties and good processability. A polymer blend can improve the membrane gas absorption performance [48]. For example, a blend can be prepared to obtain a membrane with a greater affinity for CO₂ [4]. Recently, anionic PUs introducing three different cations (imidazolium, phosphonium, and ammonium) were studied [7, 22]. Our group described the effect of polyol chemical structure and different counter cations (imidazolium, phosphonium, ammonium, and pyridinium) in CO₂ sorption capacity and CO₂/CH₄ separation performance [38]. Within this context, the aim of this work is to produce PILs blends utilizing PUs with two different polyols (Polycarbonate diol-PCD and Poly(tetramethylene ether) glycol-PTMG) into their polymer backbone and two different IL counter

cations (imidazolium and phosphonium). Thermal stability, mechanical properties, morphology, and CO₂ sorption capacity of the new blends will be presented.

Experimental

Materials

Poly(tetramethylene ether) glycol (PTMG, Mn 2000 g/mol, Sigma-Aldrich), Polycarbonate diol (PCD, Mn=2000 g/mol, Bayer, Germany), hexamethylene diisocyanate (HDI, 99%, Merck, France), dimethylol propionic acid (DMPA, 98%, Sigma-Aldrich, USA), dibutyltin dilaurate (DBTDL, Miracema Nuodex, Brasil), *N*-methyl-2-pyrrolidone (99.92%, Neon, Brasil), methylethylketone (MEK, 99%, Mallinckrodt), and potassium hydroxide (KOH, ≥85%, Sigma-Aldrich, USA) were used as received without further purification. Tetrabutylphosphonium bromide (TBPB) (98%, Sigma-Aldrich, USA) and 1-butyl-3-methylimidazolium chloride (BMIM-Cl) was synthesized as described elsewhere [49, 50]. BMIM-Cl was characterized by proton nuclear magnetic resonance (¹H-NMR) (Varian spectrophotometer, VNMRs 300 MHz), using DMSO-d₆ and 5 mm diameter glass tubes. ¹H-NMR (300 MHz, DMSO-d₆, 25 °C), δ (ppm) 1.01 (m, CH₃), 1.29 (m, CH₂CH₃), 1.83 (m, CH₂), 3.97 (s, CH₃), 4.25 (t, CH₂N), 7.79 (s, H₅), 7.91 (s, H₄), 9.48 (s, H₂).

Poly(ionic liquids) synthesis

PILs synthesis was performed in two steps as described elsewhere [20, 34]. First, PU was synthesized in a five-necked flask at 60 °C for two h using HDI as diisocyanate,

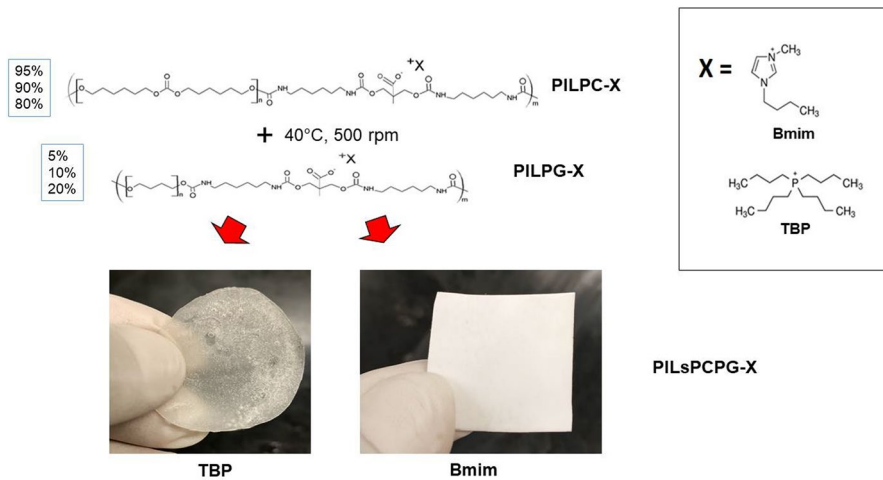


Fig. 1 Blends preparation from proposed structures of anionic PILs synthesized with different counter cations (X)

PTMG, or PCD as a polyol, DMPA diol (0.024 mol), and DBTDL (0.1 wt%) as a catalyst in MEK (25%wt.). The NCO/OH ratio of 1.05 (0.157 mol HDI/0.15 mol OH) was used. Polymer acidity was identified by titration with KOH 0.5 M. The acid number reached a value of 53 mg KOH/g (0.94 mmol of IL/g polymer) using PCD and 52 mg KOH/g (0.93 mmol of IL/g polymer) for PTMG. Second, the mixture was cooled down to 40 °C, and the IL (BMIM-Cl or TBPB) was added (molar ratio COOH/IL of 1:1). The system was maintained at 40 °C for four h under stirring to obtain the desired PIL. Films around 0.15-mm-thick were produced by casting and dried at room temperature for 72 h. PILs were labeled as PILWX, where W is polyol (PC=PCD; PG=PTMG), and X is counter cation (BMIM or TBP). For example, PILPC-TBP means PCD and TBP cation. PILs molecular weight was similar to nonionic polyurethanes (PILPC-BMIM $M_n=103.000 \text{ g mol}^{-1}$; PILPC-TBP $M_n=100.000 \text{ g mol}^{-1}$; PILPG-BMIM $M_n=112.000 \text{ g mol}^{-1}$; PILPG-TBP $M_n=133.000 \text{ g mol}^{-1}$). The use of different counter cations did not promote significant changes in the molar mass values of PLIs, as evidenced in previous studies [7, 38].

Poly(ionic liquid)s blends preparation

After PILs preparation (PU synthesis + counter cation insertion), PILs blends were produced using different PILs based on PTMG and PCD (Fig. 1). PILs were mixed by mechanical stirring (500 rpm) with a temperature of 40 °C for 90 min, according to the following proportions: 95% PILPC/5% PILPG, 90% PILPC/10% PILPG, and 80% PILPC/20% PILPG. PILs blends based on polyurethane with different polyols (PC/PG) were obtained using the ionic liquids: 1-butyl-3-methylimidazolium chloride (BMIM-Cl) and tetra-butyl phosphonium bromide (TBPB). PILs blends were labeled as PILW_nZ_nX, where W is PC, Z is PG, n is the percentage of polyol in PIL blend, and X is a counter cation (BMIM or TBP). For example, PILPC95-PG5-TBP means a blend containing 95% PILPC-TBP and 5% PILPG-TBP.

Characterization of the poly(ionic liquid)s blends

Samples structural elucidation was carried out by Fourier Transform Infrared (FTIR) spectroscopic technique. FTIR spectra were recorded on a Perkin-Elmer Spectrum 100 spectrometer scanned from 650 to 4000 cm^{-1} utilizing a UATR accessory; samples were scanned 16 times. Molecular weights were acquired from a Size Exclusion Chromatography (SEC), equipped with a Waters 1515 pump and a Waters 2412 refractive index detector, using THF as eluent at a flow rate of 1 mL/min; samples to be analyzed were dissolved in THF. Differential Scanning Calorimetry (DSC) thermograms were attained by using a TA Instrument Q20 differential scanning calorimeter in the range of -90 to 200 °C at a heating rate of 10 °C/min under a nitrogen atmosphere. Thermogravimetric Analysis (TGA) was performed using a TA Instrument SDTQ600 between 25 and 600 °C at a heating rate of 10 °C/min in a nitrogen atmosphere. Mechanical tests were carried out in triplicate based on the ASTM D822 standard technique (TA Instruments Q800 dynamic mechanical analyzer,) for determination of

Young’s modulus and stress X strain tests at 25 °C with rectangular shape films (12 mm long; 7 mm wide) with a thickness close to 0.15 mm, with 1 N/min. Field emission scanning electron microscopy (FESEM) analyses were performed in FEI Inspect F50 equipment in secondary electrons (SE) mode. AFM analyses were performed in Peak force tapping mode using a Bruker Dimension Icon PT equipped with a TAP150A probe (Bruker, resonance frequency of 150 kHz and 5 N.m⁻¹ spring constant). The equipment was calibrated prior to sample measurements. The scanned area of the images was 60×60 mm² with a resolution of 512 frames per area. The DMT Modulus map was derived from PeakForce.

Sorption measurements

CO₂ sorption capacity The pressure-decay technique was used to determine the CO₂ absorption capacity. The double-chamber cell for gas sorption is similar to the system reported in the literature [38]. A detailed description of the sorption device and the measurement procedure can be found in our previous works [7, 23, 51]. The samples (1.0–1.5 g) were placed in the sorption chamber and were degassed under vacuum (10⁻³ mbar) for one h at room temperature. The CO₂ sorption experiments were carried out at 303.15 K at different pressures at equilibrium (1 bar and 10 bar).

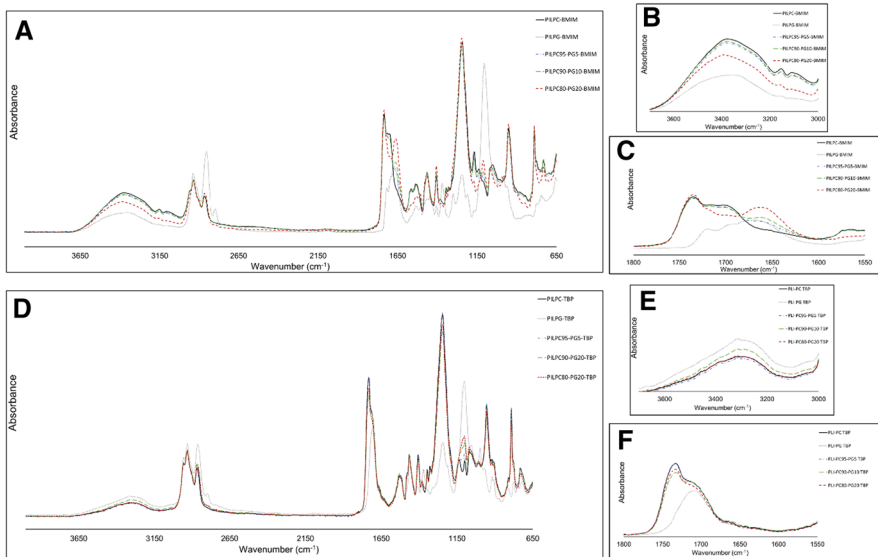


Fig. 2 FTIR spectra of PILs and PILs blends: IL BMIM **a** 650–4000 cm⁻¹, **b** 3000–3700 cm⁻¹, **c** 950–1750 cm⁻¹; IL TBP **d** 650–4000 cm⁻¹, **e** 3000–3700 cm⁻¹, and **f** 950–1750 cm⁻¹

Results and discussion

FTIR analyses showed the characteristic bands of polyurethanes, as illustrated in Fig. 2a, d. Figure 2b showed the appearance of a band associated with the vibration of the non-bonded N–H groups (3400 cm^{-1}) for samples containing counter cation BMIM [7]. Blends prepared with the counter cation BMIM also reduced the intensity of the band in 3400 cm^{-1} for higher PILPG content in blend composition (PILPC80-PG20 BMIM), which may indicate less unbounded N–H groups (Fig. 2b). The band in 3320 cm^{-1} is related to bonded N–H absorption band presented in samples containing counter cation TBP (Fig. 2e). The band in 1730 cm^{-1} is associated with “free” carbonyl groups (without hydrogen bonds), and the band in the 1700 cm^{-1} region represents carbonyl groups linked through hydrogen bonds [21, 52, 53]. As shown in Fig. 2c, there was a decrease in the intensity of the band in the region of 1700 cm^{-1} when the amount of PILPG increased by 20% for PIL BMIM blends suggesting fewer carbonyl groups linked through hydrogen bonds. For blends containing counter cation TBP, prepared with 10% and 20% of PILPG (Fig. 1f), a small reduction in the intensity of the band associated with “free” carbonyl groups was observed ($\sim 1730\text{ cm}^{-1}$). The C=O band of the carboxylic acid group (COOH) and the urethane group (NHCO) of the polymer are overlapped [7]. The changes evidenced by FTIR probably influence the thermal and mechanical behavior of the Poly(ionic liquids) blends. Spectra also showed that the conversion reaction of the isocyanate groups was complete since the 2270 cm^{-1} band related to these groups disappeared [3, 7, 53]. Other bands also appeared in the spectra: 2934 cm^{-1} (C–H of CH_2), 2859 cm^{-1} (C–H of CH_3), $1730\text{--}1702\text{ cm}^{-1}$ (urethane carbonyl groups), 1531 cm^{-1} (N–H), 1469 cm^{-1} (C–H of CH_3), 1409 cm^{-1} (COO^-), 1228 cm^{-1} (urethane C–N and C–O bonds), and 1095 cm^{-1} (C–O–C) [7, 54].

Characteristic bands of imidazolium ring C–H groups appeared around 3100 cm^{-1} in PILs, and PILs blends produced with BMIM IL [55], as shown in Fig. 2a, b. In 1095 cm^{-1} C–O–C characteristic band was more intense for PILs, and PILs blends produced with higher PG polyol content in their composition (Fig. 1). This behavior is probably due to a more significant number of ether groups

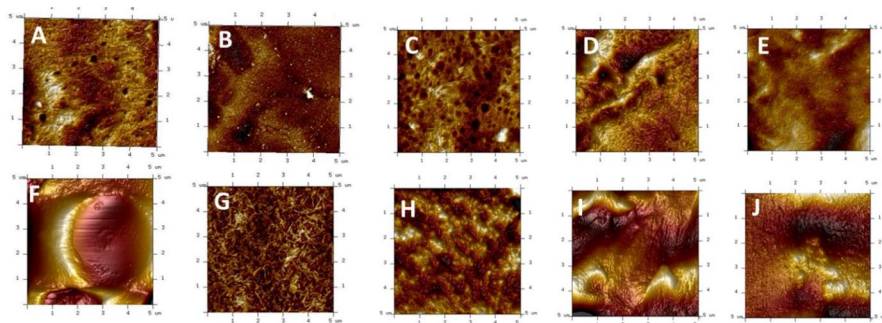


Fig. 3 AFM images (height). **A** PILPC-BMIM; **b** PILPG-BMIM; **c** PILPC95-PG5-BMIM; **d** PILPC90-PG10-BMIM; **e** PILPC80-PG20-BMIM; **f** PILPC-TBP; **g** PILPG-TBP; **h** PILPC95-PG5-TBP; **I** PILPC90-PG10-TBP, and **J** PILPC80-PG20-TBP

–C–O–C– in their structure than PILs synthesized with PC. It was also observed for all samples produced with PC polyol the characteristic band of polycarbonate bonds ($\text{O}=\text{C}-\text{O}-\text{C}$) around 800 cm^{-1} [56].

AFM images (Fig. 3) showed the surface topography for PILs and PILs blends. A typical separated microphase polyurethane structure was observed [57]. Hard domains (lighter regions) and soft domains (darker regions) showed some interaction and good distribution of the microphases [21, 58], changing according to polyol type and content (PC or PG) and IL type (BMIM or TBP). In addition, both ILs used to produce PILs, and PILs blends showed good interaction and distribution in the polymeric matrix, suggesting good connectivity between domains. It can be noticed that PILs produced with PC (Fig. 3a, f) presented a separated microphase structure with well-defined hard and soft segments. PIL BMIM blends and PIL TBP blends AFM images noticed ILs influence in the blends microphase structure. PIL BMIM blends images (Fig. 3c–e) showed that hard/soft segments distribution is more homogeneous when compared to PIL TBP blends (Fig. 3h–j), where it can be seen a higher microphase separation between segments. Yet, AFM images evidenced that with the augmentation of PILPG amount (see Fig. 3e) in PILs blend with BMIM, the miscibility of hard and soft segments was observed corroborating with FTIR founds related to a decreasing tendency in the carbonyl groups linked through hydrogen bonds. An opposite behavior was observed with TBP samples and PG content of 10 and 20%. A reduction in the band intensity associated with "free" carbonyl groups was observed by FTIR corroborating microphase separation (see Fig. 3i, j).

PILs and PILs blend SEM images are shown in Fig. 4. PILPG samples (Fig. 4b, g) presented a smooth and non-porous surface. PILs blends exhibited a mixture of each PIL characteristics. Clearly, when the amount of PILPG increased in the samples (Fig. 4e, j), PILs blends surfaces became smoother and less porous. On the other hand, PILs blends surfaces with lower concentrations of PILPG (Fig. 4c, h) were porous and rough. Rough and porous membranes could provide a larger specific surface and higher CO_2 sorption capacity [33].

In relation to DSC experiments, PILs and PILs blends also exhibited an endothermic peak related to the melting temperature (T_m) of the PU crystalline

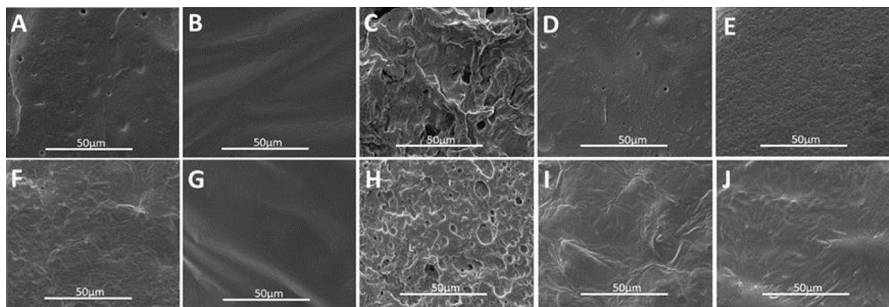


Fig. 4 FESEM micrographs. **a** PILPC-BMIM; **b** PILPG-BMIM; **c** PILPC95-PG5-BMIM; **d** PILPC90-PG10-BMIM; **e** PILPC80-PG20-BMIM; **f** PILPC-TBP; **g** PILPG-TBP; **h** PILPC95-PG5-TBP; **i** PILPC90-PG10-TBP, and **j** PILPC80-PG20-TBP

Table 1 DSC results for PLIs and PLIs blends

Sample	T_c (°C)	T_g (°C)	T_m (°C)	ΔH_c (J/g)	ΔH_m (J/g)
PILPC-BMIM	–	–43.65	42.94	–	9.552
PILPG-BMIM	–23.71	–	22.06	26.64	21.44
PILPC95-PG5-BMIM	–	–44.1	43.6	–	9.2
PILPC90-PG10-BMIM	–	–45.9	42.7	–	8.8
PILPC80-PG20-BMIM	–	–45.8	43.8	–	10.5
PILPC-TBP	–	–49.32	41.69	–	11.25
PILPG-TBP	–23.34	–	21.08	27.68	21.06
PILPC95-PG5-TBP	–	–51.9	42.1	–	8.3
PILPC90-PG10-TBP	–19.7	–51.0	1=19.3 2=41.4	0.9	1=0.7 2=4.5
PILPC80-PG20-TBP	–26.7	–52.9	1=19.4 2=41.4	1.9	1=2.0 2=3.2

microphase characteristic of PCD or PTMG polyol [7, 59], values are shown in Table 1. The T_m of crystalline microphase and crystallization enthalpies had no significant variation from PILs-BMIM blends to the starting PILPC-BMIM.

Glass transition temperature (T_g) of PILPC-TBP was lower when compared to PILPC-BMIM indicating a better microphase separation [21, 58] when using TBP as counter cation, corroborating the AFM results. DSC results evidenced that T_g values tend to decrease with the increase in the PG concentration in PILs blends being more important when TBP is the counter cation. This result indicates that with PG increasing in PILs blends composition, an increase in microphase separation occurs, as evidenced by AFM images and FTIR and previously discussed. A decrease in PILs blends T_g values suggests a greater microphase separation resulting in more flexible polymer chains when compared to PILs [60]. PILs blends with higher amounts of PG (10% and 20%) presented two peaks of melting temperature of the crystalline microphase. This phenomenon was only observed for PLI blends with LI TBP suggesting that the IL may be acting as a plasticizer [61]. Other works demonstrated the appearance of two T_m peaks for blends produced with plasticizing agents [62, 63]. It can be highlighted that when working with the IL TBP, a larger molecule when compared to the IL BMIM, T_g values were lower, suggesting an increase in mobility and flexibility of polymer chains. Cations with bulky ions tend to decrease the T_g values of the materials [64].

PILs and PILs blend thermal stability were analyzed by TGA (see Fig. 5 and Table 2). Samples containing the IL BMIM presented two typical thermal events (Fig. 5). The first thermal event ($T_{\text{onset}1}$) is related to the hard polyurethane segment breaking urethane bonds [7, 38, 65, 66]. The second thermal event is commonly associated with polyol (PC or PG). soft segments decomposition [7, 38, 67, 68]. Samples produced using the IL TBP exhibited an additional thermal event ($T_{\text{onset}3}$) probably due to a change in chain arrangement associated with the IL TBP and hydrogen bonds, as corroborated by AFM images and FTIR results.

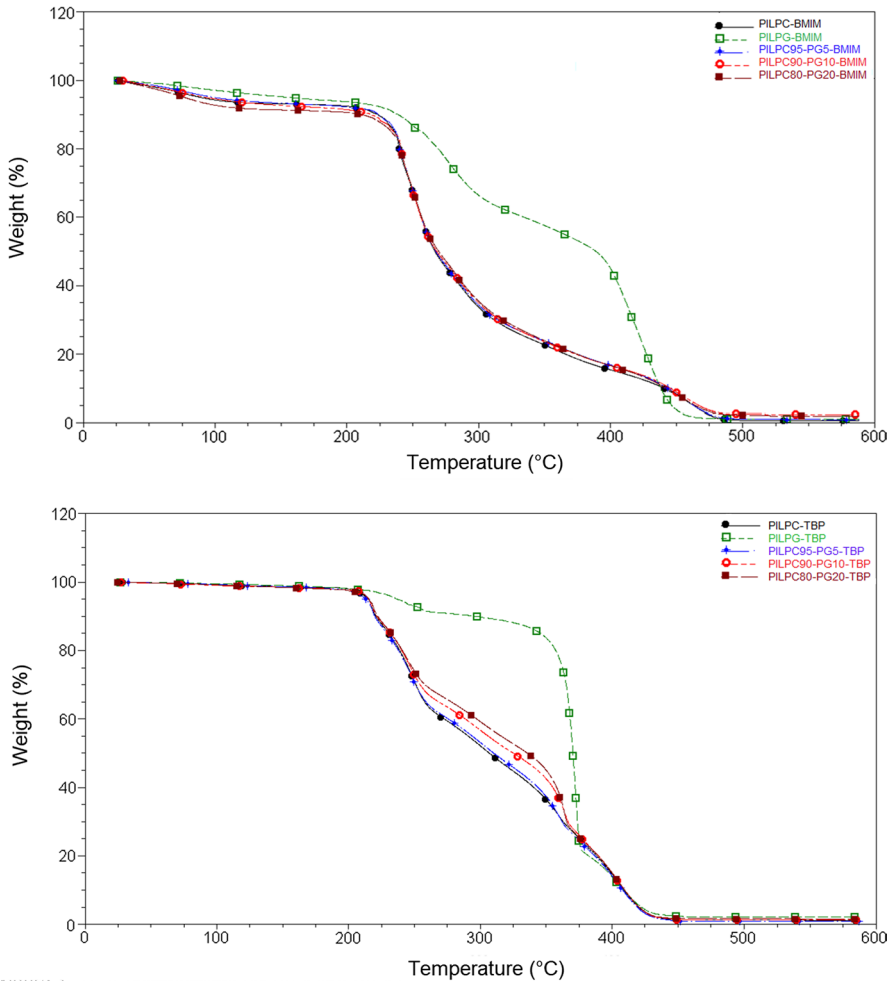


Fig. 5 TGA thermograms for PILs and PILs blends

Table 2 TGA results for PILs and PILs blends

Sample	T_{onset1} (°C)	T_{onset2} (°C)	T_{onset3} (°C)
PILPC-BMIM	235	440	–
PILPG-BMIM	246	399	–
PILPC95-PG5-BMIM	235	434	–
PILPC90-PG10-BMIM	233	429	–
PILPC80-PG20-BMIM	231	426	–
PILPC-TBP	219	350	395
PILPG-TBP	226	364	388
PILPC95-PG5-TBP	224	349	394
PILPC90-PG10-TBP	222	352	389
PILPC80-PG20-TBP	219	355	384

Table 3 DMA data of PILs and PILs blends

Sample	Young modulus (MPa)	Stress (MPa)	Strain (%)
PILPC-BMIM	5 ± 1	2 ± 0.2	150 ± 8
PILPG-BMIM	0.3 ± 0.1	0.1 ± 0.02	125 ± 30
PILPC95-PG5-BMIM	4 ± 0.5	1 ± 0.1	135 ± 13
PILPC90-PG10-BMIM	2 ± 0.3	0.6 ± 0.1	135 ± 22
PILPC80-PG20-BMIM	3 ± 0.4	0.7 ± 0.2	143 ± 15
PILPC-TBP	12 ± 2.0	2 ± 0.2	157 ± 2
PILPG-TBP	0.5 ± 0.1	0.2 ± 0.05	133 ± 5
PILPC95-PG5-TBP	11 ± 1.5	1.6 ± 0.2	156 ± 2.5
PILPC90-PG10-TBP	9 ± 1.0	1.8 ± 0.1	151 ± 2
PILPC80-PG20-TBP	7 ± 0.8	1.5 ± 0.06	156 ± 3

ILs thermal decompositions usually occur between 200 to 350 °C, implying that IL decomposition may happen in both stages of PILs and PILs blends degradation [7, 38, 69, 70]. It is noteworthy that blends formation did not significantly change thermal stability when compared to PILs (Table 2). PILs blends showed acceptable thermal stability to be used as membranes for CO₂ sorption.

Table 3 shows mechanical analysis results for PILs and PLIs blends produced with ILs BMIM and TBP. DMA stress X strain curves (Fig. 6) showed that PC-based PILs materials were more rigid than PG-based PILs, probably because PC forms stronger hydrogen bonds between flexible segments [56]. FTIR results demonstrated that samples prepared with PC presented more hydrogen bonds than samples prepared with PG. ILs inserted in polymeric structures can act as plasticizers, increasing polymer chains flexibility and affecting polymers Young's modulus [38]. PILs-BMIM and PILs-BMIM blends showed lower Young's modulus values, probably due to interactions between imidazolium ring and PU chains, corroborating with FTIR results [38]. PILs-TBP and PILs-TBP blends exhibited high Young's modulus results, which can be associated with hydrogen bonding between TBP and PU chains as showed in FTIR analysis. In summary, physical properties and morphology of polymeric materials modified with ILs can be designed through ILs chemical structure [71, 72].

PILs blends mechanical properties were influenced by the PC quantity used to form the samples. As PC amount increased, Young's modulus increased as well, resulting in a rigid PIL blend. PILs blend composition was a pivotal factor in this analysis (see Table 3). PILPC95-PG5-TBP presented superior mechanical properties related to PILPC90-PG10-TBP and PILPC80-PG20-TBP. Similar behavior occurred for samples prepared with counter cation imidazolium (BMIM). PILs blends with PC present many polar groups promoting more interactions between PU microphases resulting in mechanically resistant materials [38]. PILPC95-PG5-TBP blend showed better mechanical properties when compared to the PILPC95-PG5-BMIM blend.

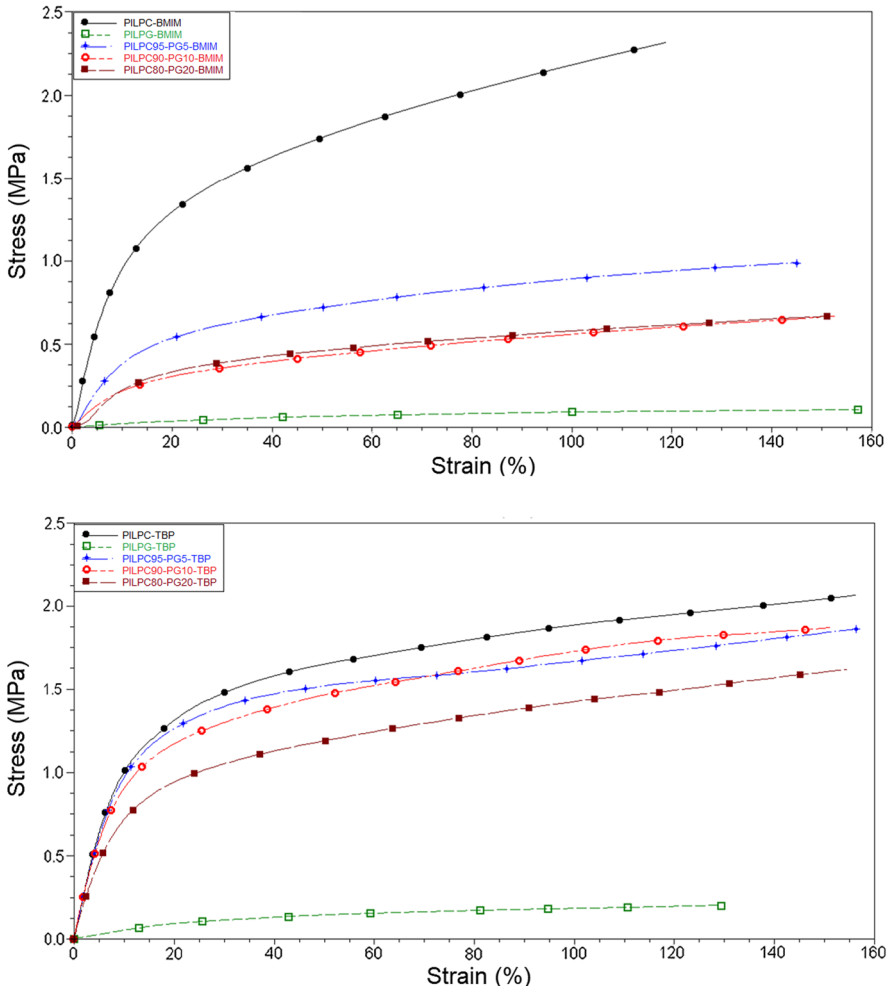


Fig. 6 Stress/strain curves for developed PILs and PILs blend films

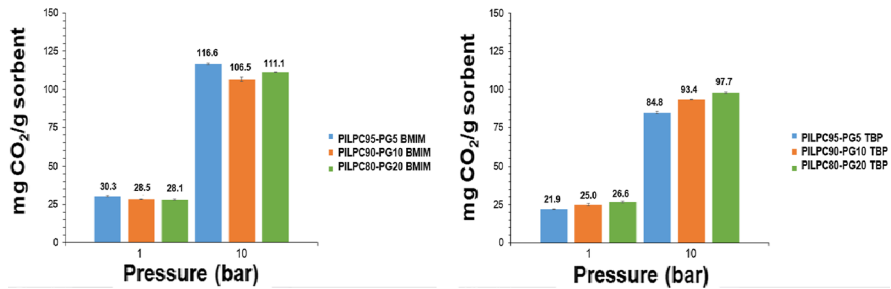


Fig. 7 PILs blend CO₂ sorption at different pressures (1 and 10 bar) and constant temperature (303.15 K)

CO₂ sorption results for PILs and PILs blends are presented in Fig. 7. Data collected in sorption analyses showed typical behavior of physical sorbents (no chemical reaction occurred). Sorption increased as CO₂ partial pressure increased [7, 73]. CO₂ affinity in a polymer is associated with interactions between CO₂ and polymer chain polar groups [7, 74, 75]. Previous works reported this behavior in pristine PU; CO₂ solubility increased as the content of polar groups increased in the polymer at 10 bar and 30 °C (PU-PG=23.0 mgCO₂/g [7]; PU-PC=40.1 mgCO₂/g [38]). In PILs, CO₂ solubility is mainly influenced by ionization. CO₂ sorption capacity increased with polymer structure ionization. Bernard et al. [38] showed that PILs had a higher CO₂ sorption capacity when adding different ILs (PILPC-TBP=45.3 mgCO₂/g at 10 bar and 30 °C; PILPC-BMIM=46.1 mgCO₂/g to 10 bar and 30 °C). PILs blends synthesized from two different polyols (PC and PTMG) positively influenced CO₂ sorption capacity results compared to PILs. As shown in Fig. 7a, all samples prepared with IL BMIM showed higher CO₂ sorption values at 10 bar and 30 °C (PILPC95-PG5-BMIM=116.6 mgCO₂/g; PILPC90-PG10-BMIM=106.5 mgCO₂/g; PILPC80-PG20-BMIM=111.1 mgCO₂/g) when compared to previous studies. Samples produced with the IL TBP also increased CO₂ sorption capacity at 10 bar and 30 °C when compared to the materials already reported in the literature (PILPC95-PG5-TBP=84.8 mgCO₂/g; PILPC90-PG10-TBP=93.4 mgCO₂/g; PILPC80-PG20-BMIM=97.7 mgCO₂/g). The best performance of the IL BMIM may be associated with a porous morphology showed by

Table 4 Comparison of PILs blends different PILs in terms of CO₂ sorption

PIL	CO ₂ sorption (mg/g)	Conditions (P, T)	Ref
[PVBIT] ^a	3.05	0.79 bar, 295.15 K	[30]
[PVBIH] ^b	3.22	0.79 bar, 295.15 K	[30]
P[(AMIM][BF4-AN] ^c	14.30	1 bar, 273.15 K	[6]
P6 [BIEMA][Br] ^d	3.34	1 bar, 278.15 K	[36]
P6[BIEMA][acetate] ^e	12.46	1 bar, 278.15 K	[36]
P[VBTEA][PF6] ^f	14.04	1 bar, 278.15 K	[76]
PIL-8.1.BF4	24.76	1 bar, 273 K	[3]
PU-TBP	15.70	0.82 bar, 303.15 K	[7]
PU-TAB	16.10	0.82 bar, 303.15 K	[7]
PILPC-TBP	21.4	0.8 bar, 303.15 K	[38]
PILPC95-PG5-BMIM	30.3	1 bar, 303.15 K	This study
PLIPC80-PG20 TBP	26.6	1 bar, 303.15 K	This study

^aPoly[1-(4-vinylbenzyl)-3-butylimidazolium tetrafluoroborate]

^bPoly[(1-(4-vinylbenzyl)- 3-butylimidazolium hexafluorophosphate]

^cPoly(ionic liquid)s based on the copolymer of 1-allyl-3-methylimidazolium tetrafluoroborate and acrylonitrile

^dPoly[2-(1-butylimidazolium-3-yl)ethyl methacrylate bromide]

^ePoly[2-(1-butylimidazolium-3-yl)ethyl methacrylate acetate]

^fPoly(4-vinylbenzyltriethylammonium hexafluorophosphate)

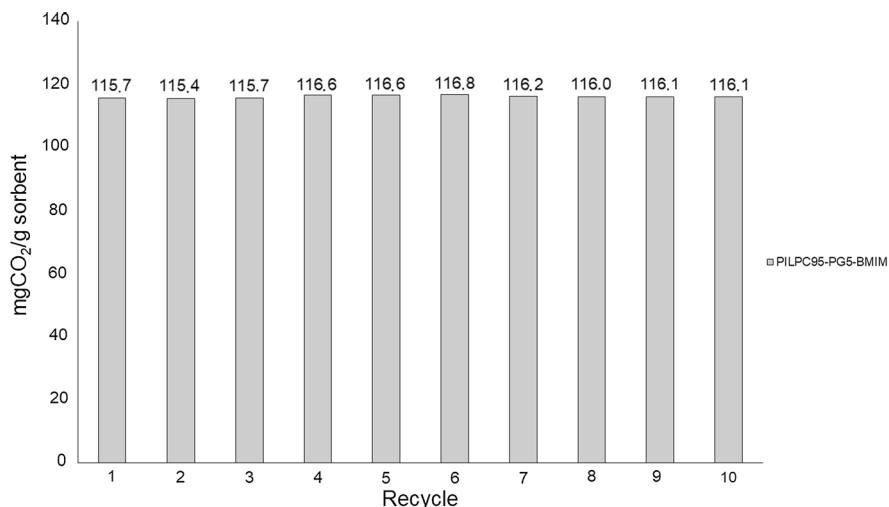


Fig. 8 CO₂ sorption/desorption tests for PILPC95-PG5-BMIM

SEM (Fig. 4c–e). At the same time, the CO₂ sorption capacity of IL TBP may be related to the weak cation–anion coordination, as previously investigated [38]. The higher occurrence of hydrogen bonds when TBP is the counter cation comparing to BMIM (see FTIR analysis) somehow can be interfering in the CO₂ sorption capacity by competing with the CO₂ by polar sites.

Table 4 shows a comparative study of the CO₂ sorption capacity of this work with several different types of PLIs described in the literature. At comparable temperatures and pressures, performance data showed that CO₂ sorption capacity for our PLIs is higher when compared to reported PILs.

Recyclability is a crucial factor when developing new sorbents. CO₂ sorption for sample PILPC95-PG5-BMIM was reversible for the ten consecutive cycles (Fig. 8). Through these results, it can be seen that the sample PILPC95-PG5-BMIM had high stability and reuse capacity in CO₂ capture processes.

Conclusions

This study reveals new PILs blends with high thermal and mechanical performance for low cost CO₂ sorbents design. Aiming to evaluate how ILs and polyol structure influence PILs blends structure, thermal and mechanical properties, and CO₂ sorption performance, two different ILs counter cations (imidazolium and phosphonium) and polyols (PC and PG) were tested. AFM analysis evidenced the ILs influence in the PLIs blends microphase structure. Yet, the PLIs blends distribution of hard and soft segments can be adjusted by controlling polyol amounts and type (PC and PG) in samples, designing mechanical and thermal properties, and CO₂ sorption capacity. All obtained PILs blends presented higher CO₂ sorption values than PILs described in the literature so far. The highest CO₂ sorption capacity (116.9 mgCO₂/g

at 303.15 K and 10 bar) was obtained for polyurethane PIL blend (PLIPC95-PG5-BMIM) using imidazolium-based counter cation.

Acknowledgements The authors would like to thank PETROBRAS for financial support (Grant number: 4600578905); Sandra Einloft thanks CNPq for the research scholarship (Grant number: 2018/00372-9).

References

1. Sanz-Pérez ES, Murdock CR, Didas SA, Jones CW (2016) Direct capture of CO₂ from ambient air. *Chem Rev* 116:11840–11876
2. Zulfikar S, Sarwar MI, Mecerreyes D (2015) Polymeric ionic liquids for CO₂ capture and separation: potential, progress and challenges. *Polym Chem* 6:6435–6451
3. Morozova SM, Shaplov AS, Lozinskaya EI et al (2017) Ionic polyurethanes as a new family of poly(ionic liquid)s for efficient CO₂ capture. *Macromolecules* 50:2814–2824. <https://doi.org/10.1021/acs.macromol.6b02812>
4. Sadeghpour M, Yusoff R, Aroua MK (2017) Polymeric ionic liquids (PILs) for CO₂ capture. *Rev Chem Eng* 33:183–200. <https://doi.org/10.1515/revce-2015-0070>
5. Mecerreyes D (2011) Polymeric ionic liquids: broadening the properties and applications of poly-electrolytes. *Prog Polym Sci* 36:1629–1648
6. Zhu J, He K, Zhang H, Xin F (2012) Effect of swelling on carbon dioxide adsorption by poly(ionic liquid)s. *Adsorpt Sci Technol* 30:35–41. <https://doi.org/10.1260/0263-6174.30.1.35>
7. Bernard FL, Polesso BB, Cobalchini FW et al (2016) CO₂ capture: tuning cation-anion interaction in urethane based poly (ionic liquids). *Polymer* 102:199–208. <https://doi.org/10.1016/j.polymer.2016.08.095>
8. Dai Z, Noble RD, Gin DL et al (2016) Combination of ionic liquids with membrane technology: a new approach for CO₂ separation. *J Memb Sci* 497:1–20
9. Eftekhari A, Saito T (2017) Synthesis and properties of polymerized ionic liquids. *Eur Polym J* 90:245–272
10. Hasib-ur-Rahman M, Sijaj M, Larachi F (2010) Ionic liquids for CO₂ capture-development and progress. *Chem Eng Process Process Intensif* 49:313–322
11. Zhao Z, Dong H, Zhang X (2012) The research progress of CO₂ capture with ionic liquids. *Chin J Chem Eng* 20:120–129. [https://doi.org/10.1016/S1004-9541\(12\)60371-1](https://doi.org/10.1016/S1004-9541(12)60371-1)
12. Green O, Grubjesic S, Lee S, Firestone MA (2009) The design of polymeric ionic liquids for the preparation of functional materials. *Polym Rev* 49:339–360. <https://doi.org/10.1080/15583720903291116>
13. Yuan J, Antonietti M (2011) Poly(ionic liquid)s: polymers expanding classical property profiles. *Polymer* 52:1469–1482
14. Yuan J, Mecerreyes D, Antonietti M (2013) Poly(ionic liquid)s: an update. *Prog Polym Sci* 38:1009–1036. <https://doi.org/10.1016/j.progpolymsci.2013.04.002>
15. Lee SY, Yasuda T, Watanabe M (2010) Fabrication of protic ionic liquid/sulfonated polyimide composite membranes for non-humidified fuel cells. *J Power Sources* 195:5909–5914. <https://doi.org/10.1016/j.jpowsour.2009.11.045>
16. Li P, Zhao Q, Anderson JL et al (2010) Synthesis of copolyimides based on room temperature ionic liquid diamines. *J Polym Sci Part A Polym Chem* 48:4036–4046. <https://doi.org/10.1002/pola.24189>
17. Shaplov AS, Morozova SM, Lozinskaya EI et al (2016) Turning into poly(ionic liquid)s as a tool for polyimide modification: synthesis, characterization and CO₂ separation properties. *Polym Chem* 7:580–591. <https://doi.org/10.1039/c5py01553g>
18. Lee M, Choi UH, Salas-De La Cruz D et al (2011) Imidazolium polyesters: structure-property relationships in thermal behavior, ionic conductivity, and morphology. *Adv Funct Mater* 21:708–717. <https://doi.org/10.1002/adfm.201001878>
19. Bhavsar RS, Kumbharkar SC, Rewar AS, Kharul UK (2014) Polybenzimidazole based film forming polymeric ionic liquids: synthesis and effects of cation-anion variation on their physical properties. *Polym Chem* 5:4083–4096. <https://doi.org/10.1039/c3py01709e>

20. Kumbharkar SC, Bhavsar RS, Kharul UK (2014) Film forming polymeric ionic liquids (PILs) based on polybenzimidazoles for CO₂ separation. *RSC Adv* 4:4500–4503. <https://doi.org/10.1039/c3ra44632h>
21. Gao R, Zhang M, Wang SW et al (2013) Polyurethanes containing an imidazolium diol-based ionic-liquid chain extender for incorporation of ionic-liquid electrolytes. *Macromol Chem Phys* 214:1027–1036. <https://doi.org/10.1002/macp.201200688>
22. Magalhães TO, Aquino AS, Vecchia FD et al (2014) Syntheses and characterization of new poly(ionic liquid)s designed for CO₂ capture. *RSC Adv* 4:18164–18170. <https://doi.org/10.1039/c4ra00071d>
23. Fernández M, Carreño LÁ, Bernard F et al (2016) Poly(ionic liquid)s nanoparticles applied in CO₂ capture. *Macromol Symp* 368:98–106. <https://doi.org/10.1002/masy.201500148>
24. Matsumoto K, Endo T (2011) Synthesis of networked polymers by copolymerization of monoepoxy-substituted lithium sulfonylimide and diepoxy-substituted poly(ethylene glycol), and their properties. *J Polym Sci Part A Polym Chem* 49:1874–1880. <https://doi.org/10.1002/pola.24614>
25. Kozo M, Takeshi E (2010) Synthesis of networked polymers with lithium counter cations from a difunctional epoxide containing poly(ethylene glycol) and an epoxide monomer carrying a lithium sulfonate salt moiety. *J Polym Sci Part A Polym Chem* 48:3113–3118. <https://doi.org/10.1002/pola.24092>
26. Matsumoto K, Endo T (2013) Design and synthesis of ionic-conductive epoxy-based networked polymers. *Reactiv Funct Polym* 73:278–282. <https://doi.org/10.1016/j.REACTFUNCTPOLYM.2012.04.0129>
27. Tang J, Shen Y, Radosz M, Sun W (2009) Isothermal carbon dioxide sorption in poly(ionic liquid)s. *Ind Eng Chem Res* 48:9113–9118. <https://doi.org/10.1021/ie900292p>
28. Tang J, Tang H, Sun W et al (2005) Low-pressure CO₂ sorption in ammonium-based poly(ionic liquid)s. *Polymer* 46:12460–12467. <https://doi.org/10.1016/j.polymer.2005.10.082>
29. Tang J, Tang H, Sun W et al (2005) Poly(ionic liquid)s as New Materials for CO₂. *Absorption* 43(22):5477–5489. <https://doi.org/10.1002/pola.21031>
30. Tang J, Sun W, Tang H et al (2005) Enhanced CO₂ absorption of poly(ionic liquid)s. *Macromolecules* 38:2037–2039. <https://doi.org/10.1021/ma047574z>
31. Mineo PG, Livoti L, Giannetto M et al (2009) Very fast CO₂ response and hydrophobic properties of novel poly(ionic liquid)s. *J Mater Chem* 19:8861–8870. <https://doi.org/10.1039/b912379b>
32. Samadi A, Kemmerlin RK, Husson SM (2010) Polymerized ionic liquid sorbents for CO₂ separation. *Energy Fuels* 24:5797–5804. <https://doi.org/10.1021/ef101027s>
33. Xiong YB, Wang H, Wang YJ, Wang RM (2012) Novel imidazolium-based poly(ionic liquid)s: preparation, characterization, and absorption of CO₂. *Polym Adv Technol* 23:835–840. <https://doi.org/10.1002/pat.1973>
34. Bhavsar RS, Kumbharkar SC, Kharul UK (2012) Polymeric ionic liquids (PILs): effect of anion variation on their CO₂ sorption. *J Memb Sci* 389:305–315. <https://doi.org/10.1016/j.memsci.2011.10.042>
35. Wilke A, Yuan J, Antonietti M, Weber J (2012) Enhanced carbon dioxide adsorption by a mesoporous poly(ionic liquid). *ACS Macro Lett* 1:1028–1031. <https://doi.org/10.1021/mz3003352>
36. Privalova EI, Karjalainen E, Nurmi M et al (2013) Imidazolium-based poly(ionic liquid)s as new alternatives for CO₂ capture. *Chemsuschem* 6:1500–1509. <https://doi.org/10.1002/cssc.201301020>
37. Bernard FL, Polesso BB, Cobalchini FW et al (2017) Hybrid alkoxy silane-functionalized urethane-imide-based poly(ionic liquid)s as a new platform for carbon dioxide capture. *Energy Fuels* 31:9840–9849. <https://doi.org/10.1021/acs.energyfuels.7b02027>
38. Bernard FL, dos Santos LM, Schwab MB et al (2019) Polyurethane-based poly(ionic liquid)s for CO₂ removal from natural gas. *J Appl Polym Sci* 136:4–11. <https://doi.org/10.1002/app.47536>
39. Supasitmongkol S, Styring P (2010) High CO₂ solubility in ionic liquids and a tetraalkylammonium-based poly(ionic liquid). *Energy Environ Sci* 3:1961–1972. <https://doi.org/10.1039/c0ee00293c>
40. Shaplov AS, Marcilla R, Mecerreyes D (2015) Recent advances in innovative polymer electrolytes based on poly(ionic liquid)s. *Electrochim Acta* 175:18–34. <https://doi.org/10.1016/j.electacta.2015.03.038>
41. Bara JE, Gin DL, Noble RD (2008) Effect of anion on gas separation performance of polymer-room-temperature ionic liquid composite membranes. *Ind Eng Chem Res* 47:9919–9924. <https://doi.org/10.1021/ie801019x>

42. Bara JE, Gabriel CJ, Hatakeyama ES et al (2008) Improving CO₂ selectivity in polymerized room-temperature ionic liquid gas separation membranes through incorporation of polar substituents. *J Memb Sci* 321:3–7. <https://doi.org/10.1016/j.memsci.2007.12.033>
43. Baker RW, Low BT (2014) Gas separation membrane materials: a perspective. *Macromolecules* 47:6999–7013. <https://doi.org/10.1021/ma501488s>
44. Sanders DF, Smith ZP, Guo R et al (2013) Energy-efficient polymeric gas separation membranes for a sustainable future: a review. *Polymer* 54:4729–4761. <https://doi.org/10.1016/j.polymer.2013.05.075>
45. Zhang Y, Sunarso J, Liu S, Wang R (2013) Current status and development of membranes for CO₂/CH₄ separation: a review. *Int J Greenh Gas Control* 12:84–107. <https://doi.org/10.1016/j.ijggc.2012.10.009>
46. Reijerkerk SR, Knoef MH, Nijmeijer K, Wessling M (2010) Poly(ethylene glycol) and poly(dimethyl siloxane): combining their advantages into efficient CO₂ gas separation membranes. *J Memb Sci* 352:126–135. <https://doi.org/10.1016/j.memsci.2010.02.008>
47. Hosseini SS, Teoh MM, Chung TS (2008) Hydrogen separation and purification in membranes of miscible polymer blends with interpenetration networks. *Polymer* 49:1594–1603. <https://doi.org/10.1016/j.polymer.2008.01.052>
48. Ben Hamouda S, Nguyen QT, Langevin D, Roudesli S (2010) Poly(vinylalcohol)/poly(ethyleneglycol)/poly(ethyleneimine) blend membranes—Structure and CO₂ facilitated transport. *Comptes Rendus Chim* 13:372–379. <https://doi.org/10.1016/j.crci.2009.10.009>
49. Welton T (1999) Room-temperature ionic liquids. solvents for synthesis and catalysis. *Chem Rev* 99:2071–2083. <https://doi.org/10.1021/cr980032t>
50. Jain N, Kumar A, Chauhan SMS (2005) Metalloporphyrin and heteropoly acid catalyzed oxidation of C=NOH bonds in an ionic liquid: biomimetic models of nitric oxide synthase. *Tetrahedron Lett* 46:2599–2602. <https://doi.org/10.1016/j.tetlet.2005.02.088>
51. Bernard FL, Duczinski RB, Rojas MF et al (2018) Cellulose based poly(ionic liquids): tuning cation-anion interaction to improve carbon dioxide sorption. *Fuel* 211:76–86. <https://doi.org/10.1016/j.fuel.2017.09.057>
52. Williams SR, Wang W, Winey KI, Long TE (2008) Synthesis and morphology of segmented poly(tetramethylene oxide)-based polyurethanes containing phosphonium salts. *Macromolecules* 41:9072–9079. <https://doi.org/10.1021/ma801942f>
53. Sadeghi M, Semsarzadeh MA, Barikani M, Ghalei B (2011) Study on the morphology and gas permeation property of polyurethane membranes. *J Memb Sci* 385–386:76–85. <https://doi.org/10.1016/j.memsci.2011.09.024>
54. Zhu R, Wang Y, Zhang Z et al (2016) Synthesis of polycarbonate urethane elastomers and effects of the chemical structures on their thermal, mechanical and biocompatibility properties. *Heliyon*. <https://doi.org/10.1016/j.heliyon.2016.e00125>
55. Xi T, Tang L, Hao W et al (2018) Morphology and pervaporation performance of ionic liquid and waterborne polyurethane composite membranes. *RSC Adv* 8:7792–7799. <https://doi.org/10.1039/c7ra13761c>
56. Chang MT, Lee JY, Rwei SP et al (2017) Effects of NCO/OH ratios and polyols during polymerization of water-based polyurethanes on polyurethane modified polylactide fabrics. *Fibers Polym* 18:203–211. <https://doi.org/10.1007/s12221-017-6382-x>
57. Liu L, Zheng Z, Gu C, Wang X (2010) The poly(urethane-ionic liquid)/multi-walled carbon nanotubes composites. *Compos Sci Technol* 70:1697–1703. <https://doi.org/10.1016/j.compscitech.2010.06.007>
58. Zhang M, Hemp ST, Zhang M et al (2014) Water-dispersible cationic polyurethanes containing pendant trialkylphosphoniums. *Polym Chem* 5:3795–3803. <https://doi.org/10.1039/c3py01779f>
59. Jime EJ (2011) Viscoelasticity of combined thermally insensitive terpolyacrylamides. *Polym Eng Sci* 51:2473–2482. <https://doi.org/10.1002/pen.22015>
60. Talakesh MM, Sadeghi M, Chenar MP, Khosravi A (2012) Gas separation properties of poly(ethylene glycol)/poly(tetramethylene glycol) based polyurethane membranes. *J Memb Sci* 415–416:469–477. <https://doi.org/10.1016/j.memsci.2012.05.033>
61. Tomé LC, Marrucho IM (2016) Ionic liquid-based materials: a platform to design engineered CO₂ separation membranes. *Chem Soc Rev* 45:2785–2824. <https://doi.org/10.1039/c5cs00510h>
62. Signori F, Boggioni A, Righetti MC et al (2015) Evidences of transesterification, chain branching and cross-linking in a biopolyester commercial blend upon reaction with dicumyl peroxide in the melt. *Macromol Mater Eng* 300:153–160. <https://doi.org/10.1002/mame.201400187>

63. Lins LC, Livi S, Duchet-Rumeau J, Gérard J-F (2015) Phosphonium ionic liquids as new compatibilizing agents of biopolymer blends composed of poly(butylene-adipate-co-terephthalate)/poly(lactic acid) (PBAT/PLA). *RSC Adv* 5:59082–59092. <https://doi.org/10.1039/c5ra10241c>
64. Chen M, White BT, Kasprzak CR, Long TE (2018) Advances in phosphonium-based ionic liquids and poly(ionic liquid)s as conductive materials. *Eur Polym J* 108:28–37. <https://doi.org/10.1016/j.eurpolymj.2018.08.015>
65. Fazeli N, Barikani M, Barikani M (2013) Study on thermal properties of polyurethane-urea elastomers prepared with different dianiline chain extenders. *J Polym Eng* 33:87–94. <https://doi.org/10.1515/polyeng-2012-0137>
66. Liu B, Tian H, Zhu L (2015) Structures and properties of polycarbonate modified polyether-polyurethanes prepared by transurethane polycondensation. *J Appl Polym Sci* 132:1–8. <https://doi.org/10.1002/app.42804>
67. Dai Z, Ansaloni L, Gin DL et al (2017) Facile fabrication of CO₂ separation membranes by cross-linking of poly(ethylene glycol) diglycidyl ether with a diamine and a polyamine-based ionic liquid. *J Memb Sci* 523:551–560. <https://doi.org/10.1016/j.memsci.2016.10.026>
68. Pashaei S, Siddaramaiah SAA (2010) Thermal degradation kinetics of polyurethane/organically modified montmorillonite clay nanocomposites by TGA. *J Macromol Sci Part A Pure Appl Chem* 47:777–783. <https://doi.org/10.1080/10601325.2010.491756>
69. Cao Y, Mu T (2014) Comprehensive investigation on the thermal stability of 66 ionic liquids by thermogravimetric analysis. *Ind Eng Chem Res* 53:8651–8664. <https://doi.org/10.1021/ie5009597>
70. Hao Y, Peng J, Hu S et al (2010) Thermal decomposition of allyl-imidazolium-based ionic liquid studied by TGA-MS analysis and DFT calculations. *Thermochim Acta* 501:78–83. <https://doi.org/10.1016/j.tca.2010.01.013>
71. Livi S, Bugatti V, Soares BG, Duchet-Rumeau J (2014) Structuration of ionic liquids in a poly(butylene-adipate-co-terephthalate) matrix: its influence on the water vapour permeability and mechanical properties. *Green Chem* 16:3758–3762. <https://doi.org/10.1039/c4gc00969j>
72. Park KI, Xanthos M (2009) A study on the degradation of polylactic acid in the presence of phosphonium ionic liquids. *Polym Degrad Stab* 94:834–844. <https://doi.org/10.1016/j.polymdegradstab.2009.01.030>
73. Ahmady A, Hashim MA, Aroua MK (2011) Absorption of carbon dioxide in the aqueous mixtures of methyldiethanolamine with three types of imidazolium-based ionic liquids. *Fluid Phase Equilib* 309:76–82. <https://doi.org/10.1016/j.fluid.2011.06.029>
74. Gabrienko AA, Ewing AV, Chibiryaev AM et al (2016) New insights into the mechanism of interaction between CO₂ and polymers from thermodynamic parameters obtained by in situ ATR-FTIR spectroscopy. *Phys Chem Chem Phys* 18:6465–6475. <https://doi.org/10.1039/c5cp06431g>
75. Tomasko DL, Li H, Liu D et al (2003) A review of CO₂ applications in the processing of polymers. *Ind Eng Chem Res* 42:6431–6456. <https://doi.org/10.1021/ie030199z>
76. Yu G, Hu X, Wang X et al (2014) Characterization of low angle grain boundary in large sapphire crystal grown by the kyropoulos method. *J Cryst Growth* 405:59–63. <https://doi.org/10.1016/j.jcrysgro.2014.07.053>

Publisher's Note Springer Nature remains neutral with regard to jurisdictional claims in published maps and institutional affiliations.